Synthesis, characterization, thermodynamics and biological studies of binary and ternary complexes including some divalent metal ions, 2, 3-dihydroxybenzoic acid and *N*-acetylcysteine

Shella Permatasari Santoso[a], Artik Elisa Angkawijaya[b], Yi-Hsu Ju[a,*], Felycia Edi Soetaredjo[c], Suryadi Ismadji[c], Aning Ayucitra[c]

[a] *Department of Chemical Engineering, National Taiwan University of Science and Technology, Taipei 10607, Taiwan*
[b] *Institute of Plant and Microbial Biology, Academia Sinica, Taipei 11529, Taiwan*
[c] *Department of Chemical Engineering, Widya Mandala Surabaya Catholic University Kalijudan 37, Surabaya 60114, Indonesia*

A B S T R A C T

The binary complexes with the $[M(Dhba)]^-$ core and ternary complexes with $[M(Dhba)(Nac)]^{3-}$ core have been synthesized and characterized by physical and spectral analyses, where M is divalent metal (Mn^{2+}, Co^{2+}, Ni^{2+}, Cu^{2+} or Zn^{2+}) and Dhba and Nac are 2, 3-dihydroxybenzoic acid and *N*-acetylcysteine, respectively. The synthesized complexes are practical in biological applications since they are soluble in water. The synthesized complexes were found to possess enhanced antimicrobial activity, especially against *Staphylococcus aureus*, but reduced DPPH scavenging activity of Dhba. The binary and ternary complexes of Zn^{2+} were shown to possess the most remarkable properties thus their structures were further examined. Thermodynamic properties of the Zn^{2+} complexes in aqueous solution at various temperatures were also determined with an ionic strength of 0.15 mol/dm^3 NaCl.

© 2016 Taiwan Institute of Chemical Engineers. Published by Elsevier B.V. All rights reserved.

1. Introduction

Synthesis of chelate complex drugs is one of the solutions to deal with pathogenic microbes which are becoming more and more drug resistance [1,2]. Bioactive organic ligands such as amino acids, phenolic acids and alkaloids coupled with essential metals are frequently employed in chelate complex synthesis [3–6]. 2, 3-Dihydroxybenzoic acid (Dhba) is an effective phenolic compound not only with regard to its biological ability such as antioxidant, antibacterial and anti-inflammatory [7,8], but also to its ability to form stable chelate complexes with various metal ions [9–11]. Therefore, Dhba was chosen as the ligand for the synthesis of metal–ligand binary complexes in this study. Ternary chelate complexes involving mixed ligands (Dhba and *N*-acetylcysteine (Nac)) were also synthesized. Nac was chosen as the consort ligand since it has been known to play an important role as a precursor of glutathione, an important antioxidant, and also known as potential

sulfur replenishment for living organisms [12,13]. Moreover, Nac can form coordination compounds with metal ions [11,14,15].

In this study, binary and ternary complexes including Dhba, Nac and some divalent metal ions such as Mn^{2+}, Co^{2+}, Ni^{2+}, Cu^{2+} and Zn^{2+} were synthesized and characterized. The chelate complexes were initially characterized by FTIR and UV–vis spectroscopy analyses. Scavenging activity and antibacterial activity of the complexes were examined. Subsequently, binary and ternary complexes with high biological activity were further studied using elemental analysis, ^1H NMR and thermogravimetric analysis; their thermodynamic properties were also determined.

2. Experimental

2.1. Materials and instruments

Copper chloride dihydrate ($CuCl_2 \cdot 2H_2O$, 99% purity), cobalt nitrate hexahydrate ($Co(NO_3)_2 \cdot 6H_2O$, 98% purity), zinc nitrate hexahydrate ($Zn(NO_3)_2 \cdot 6H_2O$, 98% purity), Dhba ($C_7H_6O_4$, 99% purity) and Nac ($C_5H_9NO_3S$, 99% purity) were purchased from Sigma–Aldrich (St. Louis, MO); nickel chloride hexahydrate ($NiCl_2 \cdot 6H_2O$, 98% purity) was obtained from Alfa Aesar (Lancashire, UK); manganese chloride tetrahydrate ($MnCl_2 \cdot 4H_2O$, 99.8% purity) was supplied by Fisher Scientific (Bridgewater, NJ).

* Corresponding author at: Department of Chemical Engineering, National Taiwan University of Science and Technology, #43, Sec. 4, Keelung Road, Taipei 106-07, Taiwan. Fax: +886 2 27376644.

E-mail address: yhju@mail.ntust.edu.tw (Y.-H. Ju).

Sodium hydroxide (NaOH, 96% purity) was supplied by Yakuri Chemical (Kyoto, Japan). Ethanol (C_2H_6O, 95% purity) was provided by Echo Chemical (Miaoli, Taiwan). All chemicals were analytical grade and were used without further purification.

N, C, S and H analysis was performed using an Elementar Vario EL Cube analyzer (Hanau, Germany). Metal contents (Mn, Co, Ni, Cu, Zn and Na) of the complexes were determined by an ICP-AES JY 2000-2. The commercial ICP metal standard solution (1000 mg/l of metal in 0.5 mol/l HNO_3) was used as the calibrant. Chloride content was determined by using an ion chromatograph Dionex ICS-1000. FTIR spectra were recorded with a Bio-Rad FTS-3500 on KBr disc with spectra range of 400–4000 cm^{-1}. UV–vis spectra of the complexes in H_2O solvent were measured in the wavelength range of 200–500 nm by using a Jasco V-550 spectrophotometer. Conductivities of the complexes in water were measured using a Knick Konduktometer 703. Magnetic susceptibilities of powder samples at 300 K were measured using a MPMS7 Quantum Design SQUID Magnetometer. ^1H NMR spectra were measured on a Bruker AVIII-600 MHz FT-NMR in D_2O solution. Thermogravimetric analyses in the range of 30 to 900 °C were examined by using a Perkin Elmer Diamond TG/DTA. Thermodynamic properties in 0.15 mol/dm^3 NaCl ionic medium at various temperatures were measured potentiometrically under N_2 atmosphere by using a Metrohm 888 Titrando potentiometer with Ecotrode Plus pH glass electrode.

2.2. Synthesis of binary and ternary complexes

Binary complexes were synthesized by dissolving Dhba (0.16 g, 1 mmol) in 14 ml H_2O with the addition of 1 ml 95% ethanol. The ligand was allowed to dissolve by slowly adding a few drops of ±5 M NaOH solution until pH 11.0 was reached, NaOH solution was directly used without standardization. Five milliliters of 1 mmol metal salt solution (0.17 g $CuCl_2 \cdot 2H_2O$; 0.30 g $Zn(NO_3)_2 \cdot 6H_2O$; 0.24 g $NiCl_2 \cdot 6H_2O$; 0.30 g $Co(NO_3)_2 \cdot 6H_2O$; or 0.20 g $MnCl_2 \cdot 4H_2O$) was added into the solution. The pH again was adjusted to 11.0 by using ±5 M NaOH. The mixture was allowed to react for 6 h with constant stirring. Any solid in the solution was removed by filtration. The solution was freezed in −40 °C and then subjected to lyophilization. The dried complex was washed with ethanol and dried in a 50 °C oven for 4 h, then stored in a desiccator.

Ternary complexes were synthesized similarly to that of binary complexes with the addition of Nac (0.16 g, 1 mmol).

2.3. Scavenging activity

Scavenging activity of complexes was tested against the stable radical 2,2-diphenyl-1-picrylhydrazyl (DPPH) [16]. The tested complex was prepared at concentrations of 1 and 2 μg/ml. The complex was firstly dissolved in water, then methanol was added at a water to methanol ratio of 1:19 (v/v). DPPH solution was prepared at a concentration of 5×10^{-4} mol/l in aqueous solution with the same water to methanol ratio. DPPH solution (0.2 ml) was added to the prepared complex (0.8 ml). The tested complexes incubated at 37 °C for 30 min and its absorbance was measured at 517 nm against methanol blank. DPPH (0.2 ml) in methanol (0.8 ml) was used as the control. Percent DPPH inhibition was calculated as:

$$\% \text{ DPPH inhibition} = ([A_c - A_s]/A_c) \times 100 \qquad (1)$$

where A_c and A_s are the absorbance of control and the absorbance of sample, respectively. Ascorbic acid was used as the positive controls.

2.4. Antimicrobial activity

The antimicrobial potency of the complexes was tested against gram positive *Staphylococcus aureus* and gram negative *Escherichia coli*. Broth macrodilution method was used for the inhibitory activity determination [17]. Ampicilin (895.5 μg/ml potency) was used as the reference. The complex was prepared at four concentrations (100, 600, 1000 and 2000 μg/ml). The assay was performed in test tubes each containing the tested compound dissolved in *Lysogeny Broth* media. Fifteen microliters of the prepared bacteria suspension (1×10^8 cfu/ml) were injected into each tube. After incubated for 24 h at 37 °C, optical density at 600 nm wavelength (OD_{600nm}) of each sample was measured. As the growth control, 15 μl of bacteria suspension was injected into test tube containing no sample. The antimicrobial activity is expressed as %inhibition, calculated as:

$$\% \text{ inhibition} = ([I_c - I_s]/I_c) \times 100 \qquad (2)$$

where I_c is the absorbance of control and I_s is the absorbance of sample.

2.5. Thermodynamic properties

Thermodynamic properties were determined potentiometrically by titrating 50 cm^{-3} mixture of metal salts (0.001 mol/dm^3) and 0.001–0.003 mol/dm^3 of Dhba and/or Nac. The mixture was acidified to pH 2.5 by adding 0.003 mol/dm^3 HCl. The ionic strength maintained by adding 0.15 mol/dm^3 NaCl. The mixture was titrated by 0.1 mol/dm^3 carbonate free-NaOH under N_2 atmosphere until pH 11.0 was reached. Stability constant of binary complex was determined at metal to ligand ratios of 1:1, 1:2 and 1:3 while ternary complex was determined from metal to ligand ratio of 1:1:1. Stability constants were determined at 25, 45 and 55 °C. Analyses of the titration data were done by using Hyperquad2008 [18].

3. Results and discussion

Metal–ligand complexes with deprotonated species as core (specifically $[M(Dhba)]^-$ and $[M(Dhba)(Nac)]^{3-}$, for binary and ternary species respectively) were synthesized at pH 11.0. This pH was chosen for the synthesis reaction since at this pH value core species were found to exist in the highest concentration, as shown in the distribution diagram in Supplementary Data Fig. S1 for Zn^{2+} systems. The synthesized complexes were then characterized by FTIR and UV–vis spectra analyses. DPPH scavenging and antimicrobial activities of complexes were evaluated. The results of elemental analysis, conductivity and magnetic measurements of Zn^{2+} binary and ternary complexes are presented in this section while the results of other metal ions complexes are summarized in the supplementary data (Table S1).

3.1. FTIR spectra

3.1.1. Binary complexes

The characteristic main bands in IR spectra of the ligands and binary complexes are listed in Table 1, while the IR spectra are presented in the supplementary data (Figs. S2 and S3). In the absence of metal ions, Dhba possessed bands at 3240 cm^{-1} and 3048 cm^{-1} corresponding to $v(OH)$ of hydroxyl and carboxyl group, respectively. The IR spectrum of the free Dhba reveals a band at 1680 cm^{-1} due to $v(C=O)$ and $v(C-OH)$ of protonated carboxyl group, respectively. The band at 1566 cm^{-1} is attributed to the $v(C=C)$ of Dhba aromatic ring, in the complexes this band is found at 1530–1548 cm^{-1}. Several new bands can be found in the metal complex system. The first is the $v(OH)$ band at 3478–3471 cm^{-1} and 837–811 cm^{-1} regions are due to coordinated water molecule [6,19]. Two new bands at 1618–1617 cm^{-1} and 1473–1431 cm^{-1} are contributed to $v(COO^-)_{asy}$ and $v(COO^-)_{sym}$ of deprotonated carboxylic group, Δv of 145–187 cm^{-1} suggests that this group is unbounded.

Table 1
Selected IR spectra for the synthesized binary and ternary complexes.

Complex	IR spectra (cm⁻¹)															
	Binary							Ternary								
	ν(OH)	ν(C=O)	ν(COO⁻)	ν(C=C)	ν(C–OH)	ν(MO)	other	ν(NH)	ν(OH)	ν(SH)	ν(C=O)	ν(COO⁻)	ν(C=C)	ν(C–OH)	ν(MO)	Other
Ligand																
Dhba	3240 3048	1680	–	1566	1259	–	–	–	3240 3048	–	1680	–	1566	1259	–	–
Nac	–	–	–	–	–	–	–	3376 796	2810	2548	1718	–	–	1229	–	–
Complex of																
Copper	3478 811	–	1618 1451	1548	1216	477	620	755	3449 806	–	–	1548 1440	1548	1217	516	588
Zinc	3471 820	–	1618 1445	1537	1192	476	1384 1222	746	3385 810	–	–	1627 1501	1573	1214	457	1384 1254
Nickel	3477 837	–	1617 1445	1533	1196	476	621	745	3373 834	–	–	1628 1502	1565	1228	458	599
Cobalt	3478 834	–	1618 1473	1530	1191	476	1384 1251	758	3352 826	–	–	1615 1471	1580	1218	457	1384 1258
Manganese	3478 813	–	1618 1431	1530	1218	478	621	746	3371 813	–	–	1659 1492	1566	1220	457	597

The ν(C–OH) band at 1191–1218 cm⁻¹ is due to ethanol. The complex of Cu²⁺, Ni²⁺ and Mn²⁺ possessed band at 621–620 cm⁻¹ indicating the ionic Cl⁻; while for Zn²⁺ and Co²⁺ the bands at 1384 and 1251–1222 cm⁻¹ indicate the coordinated NO₃⁻ in monodentate mode [20]. The ionic groups of Cl⁻ and NO₃⁻ were originated from the type of metal salts used. The new band appeared at 477, 476, 476, 476 and 478 cm⁻¹ are attributed to ν(MO) for Cu²⁺, Zn²⁺, Ni²⁺, Co²⁺ and Mn²⁺, respectively.

3.1.2. Ternary complexes

The IR absorption bands of the ternary complexes are listed in Table 1 as well as binary complexes (the full spectra are presented in supplementary data Fig. S4). The ligand Nac ν(NH) stretching and bending vibration was observed at 3376 and 796 cm⁻¹, respectively. The stretch of ν(OH), ν(C=O) and ν(CO) bond from protonated carboxylate group produced band at 2810 cm⁻¹, 1718 cm⁻¹ and 1229 cm⁻¹ respectively. The thiol ν(SH) frequency of Nac was characterized at 2548 cm⁻¹, while in the complex this band disappeared, evidencing that this group was involved in chelation after deprotonation. The synthesized ternary complexes inherited the main spectra from both Dhba and Nac. The ν(OH) at 3449–3352 cm⁻¹ and band at 834–806 cm⁻¹ in all metal systems indicate the coordinated water molecule [6,19]. The bending of ν(NH) at 758–745 cm⁻¹ was still visible in the complexes, while the stretching of ν(NH) at higher region cannot be observed since the band is probably stacked with the ν(OH) band. Two bands at 1659–1548 cm⁻¹ and 1502–1440 cm⁻¹ are contributed to ν(COO⁻)$_{asy}$ and ν(COO⁻)$_{sym}$ of the deprotonated carboxylic group, $\Delta\nu = 108$–167 cm⁻¹ indicating the monodentate binding of the carboxylic group [6,19]. The ν(C–OH) band at 1214–1228 cm⁻¹ is due to ethanol. The ionic group Cl⁻ originated from metal salts appeared at 599–588 cm⁻¹ for Cu²⁺, Ni²⁺ and Mn²⁺, while coordinated NO₃⁻ in monodentated mode appeared at 1384 and 1258–1254 cm⁻¹ for Zn²⁺ and Co²⁺ [20]. The band which characterized the bond of ligand to metal, ν(MO) was observed at 516, 457, 458, 457 and 457 cm⁻¹ for Cu²⁺, Zn²⁺, Ni²⁺, Co²⁺ and Mn²⁺, respectively.

3.2. UV–vis spectra, conductivity and magnetic properties

Absorption spectra of the synthesized binary and ternary complexes are shown in Fig. 1. The complexes show two absorption bands at 214–230 nm and 314–360 nm which correspond to π–π^* and n–π^* bonding of the benzene ring [21]. In binary and ternary cobalt complexes, n–π^* bonding was observed at longer wavelength (370–395 nm), while for manganese complexes the absorbance of this bonding was low and cannot be observed. The absorption bands for d-orbital of the metals cannot be observed since usually these spectra have low absorbance. In particular for ternary complex of Co²⁺, the spectrum corresponding to d-orbital is observed at 499 nm which is attributed to the transition $^4A_{2g}(F) \rightarrow {}^4T_{1g}(P)$, indicating its octahedral geometry [22].

Magnetic susceptibilities (μ_{eff}) of the binary and ternary complexes were measured at 300 K and are summarized in Table S1. Low μ_{eff} values (0.69–1.00 BM for binary and 0.62–1.75 BM for ternary complexes) suggest that the complexes only have one unpaired electron, and the complexes exhibit weak paramagnetic behavior. In Zn²⁺ binary and ternary complexes, the results of μ_{eff} indicate diamagnetic behavior of the complexes. Meanwhile, Co²⁺ ternary complex exhibits higher μ_{eff} (2.38 BM) than other ternary metal complexes, this value is often observed for Co²⁺ complex with octahedral geometry and is also supported by the occurrence of the band at 499 nm in UV–vis spectra.

The molar conductivity (Λ_M) measurements gave values of 153–179 S cm²/mol for binary complexes, while for ternary complexes the values were 217–242 S cm²/mol (Table S1). Λ_M of a complex indicates the electrolyte nature of the complex. The electrolyte behavior of a complex might be due to the presence of Na⁺ ions which were involved in the formation of the complex. Higher Λ_M of a ternary complex is because it contains more Na⁺ ions than a binary complex.

3.3. Biological activities

3.3.1. DPPH scavenging activity

Scavenging activity of the complexes at concentrations of 1 and 2 mg/l were evaluated against DPPH. The tests in scavenging activity were done in triplicate. The results are summarized as the average value, and the difference between the three tests was indicated by the error bars, as shown in Fig. 2. The synthesized binary and ternary complexes did not show any increase in DPPH inhibition compared to Dhba. The possible reason is that originally Dhba inhibits DPPH by transferring H atom from −COO and *meta* −O group [23] while Nac inhibits DPPH by transferring H atom from −COO group [24]; in the formed complex H atoms of ligand which were originally inhibiting free radical formation disappeared thus inhibition activity actually decreased.

Ternary complexes have higher inhibition activity than binary complexes. The enhancement in activity is due to the addition of
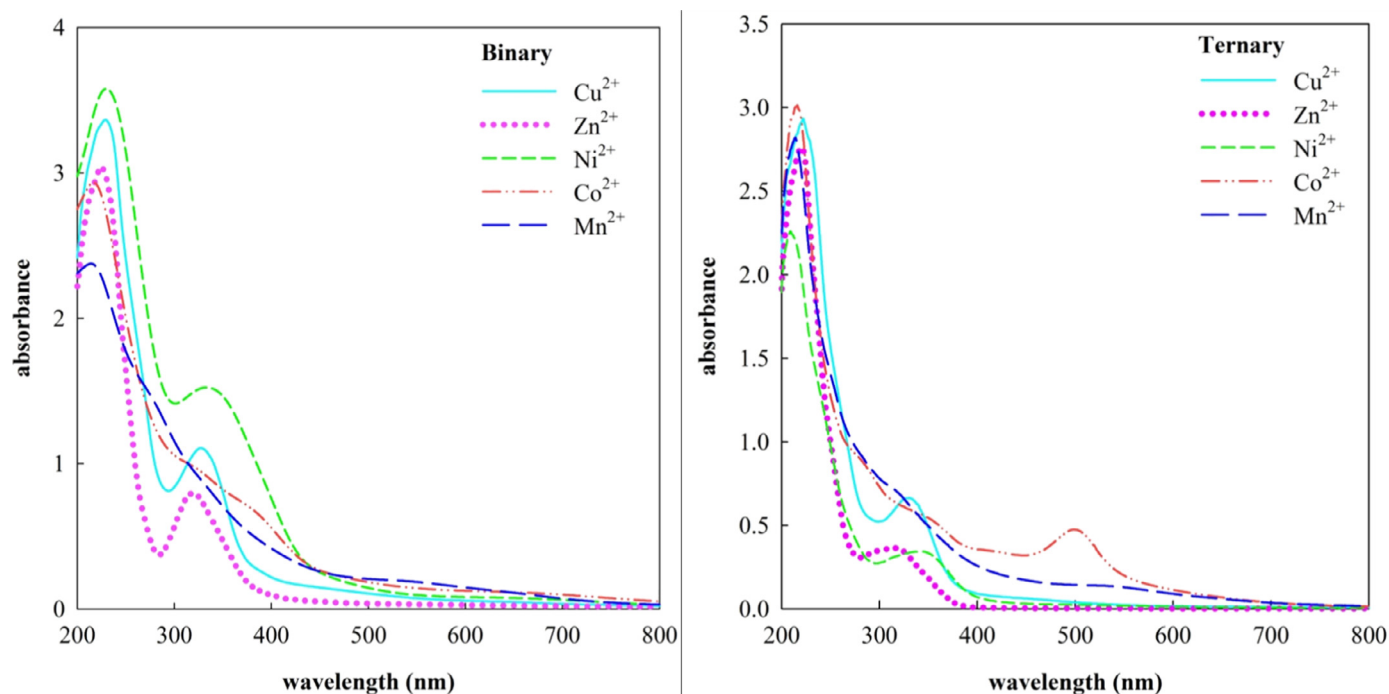
Fig. 1. Spectra of the binary and ternary complexes at concentration of 187.5 mg/l.
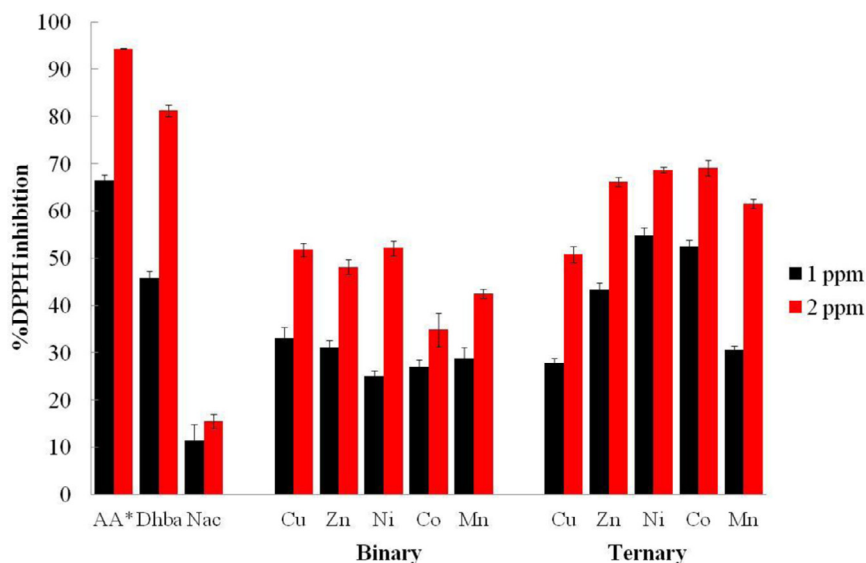

Fig. 2. DPPH scavenging activity of the complexes, *AA-ascorbic acid as the standard reference.

Nac, where amine group of Nac also contributes to bonding with DPPH through weak hydrogen bond. However for ternary complex of Cu^{2+}, the inhibition activity is lower than that of binary Cu^{2+} perhaps due to the reaction of Nac and Cu^{2+} which is known to produce free radical [25].

3.3.2. Antimicrobial activity

Antimicrobial activities of the synthesized complexes were evaluated against *E. coli* and *S. aureus*. The inhibition values are reported as Supplementary Data (Tables S2–S4). Dhba was shown to have better antimicrobial activity than Nac. For the synthesized complexes, some exhibited lower antimicrobial activity than that of Dhba. The complexes were found to be more effective in inhibiting *S. aureus*. It was found that in binary and ternary complexes, the complex of Zn possessed the highest inhibition activity against

the growth of bacteria. Thus it is worthwhile to diagnose the efficacy of zinc complexes by determining the minimum inhibitory concentration (MIC) as shown in Table 2. The complexes of zinc gave higher inhibition activity than ligand alone (especially against *S. aureus*) as indicated by the smaller MIC values.

The increase in bacterial growth inhibition of zinc complexes is perhaps due to the increase in solubility of the complexes. The solubility of Dhba in water is very low and becomes highly soluble in the form of chelate complex. The complexes were also found to be more effective to inhibit the growth of gram positive bacteria than gram negative bacteria. This is possibly due to difference in their cell walls [26,27]. As gram positive bacteria, *S. aureus* cell wall consists of thick peptidoglycan layer and plasma membrane while gram negative bacteria *E. coli* cell wall possesses an extra outer membrane layer which is high in lipid [28]. This lipid
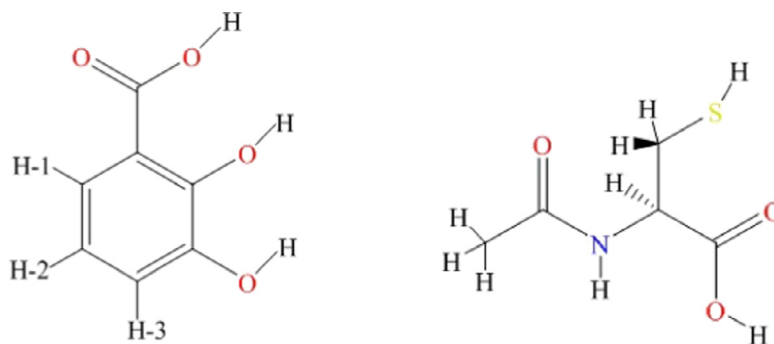
Fig. 3. Structure of ligand Dhba (left) and Nac (right).

Table 2
MIC[a] (μg/ml) of the tested compounds.

Compound	E. coli		S. aureus	
	MIC$_{50}$	MIC$_{90}$	MIC$_{50}$	MIC$_{90}$
Ampicilin	4.1	49.1	0.3	2.6
Dhba	589.8	1085.7	702.0	932.6
Nac	1293.9	>2000	>2000	>2000
Binary zinc	603.5	867.0	149.3	383.8
Ternary zinc	773.9	971.6	347.1	554.8

MIC$_{50}$ and MIC$_{90}$ are the minimum concentration requirement to inhibit 50% and 90% growth of microorganism, respectively.
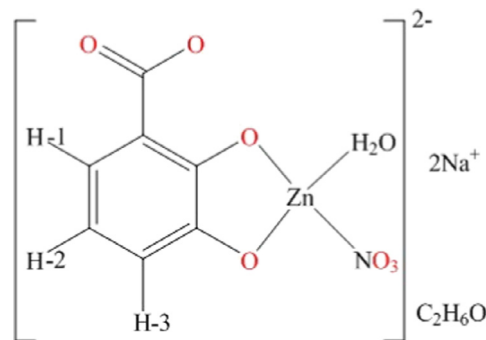

Fig. 4. Proposed structure of zinc binary complex.

containing layer lowers the permeability of the complex into the bacteria inner membrane and cause decrease in inhibition activity.

3.4. Complexes of zinc

Since the complexes of Zn show higher biological activity than other metal complexes, only Zn complexes were chosen for further characterization including elemental analysis, ^{1}H NMR spectra, and thermogravimetric analysis.

3.4.1. Binary complex of zinc

The binary complex of Zn has the chemical formula $C_9H_{11}NNa_2O_9Zn$ or $Na_2[Zn(NO_3)(C_7H_3O_4)(H_2O)]\cdot C_2H_6O$, $mw = 388.54$. It is dark green-brown in color. Elemental analysis on the complex indicated its composition as follows: C, 27.89; H, 2.84; N, 3.69; Na, 11.80; Zn, 16.52% while the calculated (theoretical) composition is: C, 27.82; H, 2.85; N, 3.61; Na, 11.83; Zn, 16.83%. The ^{1}H NMR signals of Dhba (Fig. 3) were found at δ_H 7.47 (d, 1H, H-1, $J = 6.5$ Hz), 7.16 (d, 1H, H-2, $J = 6.4$ Hz), 6.88 (t, 1H, H-3, $J = 8.0$). The binary complex signals were shifted to lower values specifically δ_H 7.12 (s, 1H, H-1), 6.82 (s, 1H, H-2), 6.61 (s, 1H, H-3), followed by new signals at δ_H 3.69 (q, 2H, CH$_2$, $J = 7.1$ Hz), 1.22 (t, 3H, CH$_3$, $J = 7.1$ Hz). The ^{1}H NMR signals are presented in Table 3, while the spectrums are presented in Figs. S5 and S6. The new ^{1}H NMR signals in the complex were observed which corresponds to ethanol molecule. The attachment of ethanol molecule may also cause the shift in v(OH) IR spectra at 3471 cm^{-1}.

As indicated in the elemental analysis, Na$^+$ molecules were involved in the formation of complex. Na$^+$ molecules seem to help neutralizing the charge of the complex, which originally has a negative charge of 2, thus isolation of the complex in solid phase is possible. Result of elemental analysis suggests that there was one N atom corresponding to NO$_3$ involved in complex formation. Thus the proposed structure of zinc binary complex is shown in Fig. 4.

3.4.2. Ternary complex of zinc

Ternary complex was found with chemical formula $C_{14}H_{18}N_2Na_4O_{12}SZn$ or $Na_4[Zn(NO_3)(C_7H_3O_4)(C_5H_7NO_3S)(H_2O)]\cdot C_2H_6O$, $mw = 595.70$. The complex has a dark pale-brown color. Elemental analysis found the composition as: C, 28.46; H, 3.06; N, 4.72; S, 5.22; Na, 15.31; Zn, 11.01% while the calculated (theoretical) one is: C, 28.23; H, 3.05; N, 4.70; S, 5.38; Na, 15.44; Zn, 10.98%. More complicated ^{1}H NMR signals were observed in ternary complex. ^{1}H NMR signals for Dhba were the same as those in the binary complex, while for Nac (Fig. 3) the signals observed are δ_H 4.66 (q, 1H, CH, $J = 4.9$ Hz), 3.02 (sep, 2H, CH$_2$, $J = 9.4$ Hz), 2.11 (s, 3H, CH$_3$). ^{1}H NMR signals for zinc ternary complex (Table 5) are δ_H 7.12–7.03 (m, 1H, H-1), 6.78 (br, 1H, H-2), 6.69–6.59 (m, 1H, H-3), 4.53 (q, 1H, CH Nac, $J = 4.1$ Hz), 3.69 (q, 2H, CH$_2$ ethanol, $J = 7.1$ Hz), 3.02–2.99 (dd, 2H, CH$_2$ Nac, $J = 8.9$ Hz), 1.60 (s, 3H, CH$_3$ Nac), 1.22 (t, 3H, CH$_3$ ethanol, $J = 7.1$ Hz). The ^{1}H NMR spectrums of Nac and ternary complex are presented in Figs. S5 and S6.

Similarly in Zn ternary complex, Na$^+$ molecules also helped neutralizing the charge of the complex, which originally has a negative charge of 4. Elemental analysis result also suggests the involvement of NO$_3$ in complex formation. Thus the structure of zinc ternary complex can be proposed as shown in Fig. 5.

3.4.3. Thermogravimetric analyses

Thermogravimetric analyses of Zn complexes were conducted in the temperature range of 30–900 °C. The thermograms are provided in Supplementary Data (Figs. S5). In Zn binary complex, the initial mass loss which is observed until 200 °C corresponds to loss of water and ethanol. Big mass loss at 280–340 °C corresponds to the decomposition of Dhba, thus residue at above 450 °C corresponds to zinc-oxide. For Zn ternary complex, the initial mass loss which was observed until 140 °C corresponds to loss of water and ethanol. Mass loss at 145–550 °C corresponds to the decomposition of ligand Nac along with Dhba and zinc-oxide residue was left at temperatures above 550 °C.

Table 3
Selected ^{1}H NMR data of zinc binary and ternary complex.

Proton chemical shift[a] (assignment)[b]					
Ligand		Zn binary complex		Zn ternary complex	
7.47	(d, 1H, H-1 Dhba)	7.12	(s, 1H, H-1)	7.12–7.03	(m, 1H, H-1 Dhba)
7.16	(d, 1H, H-2 Dhba)	6.82	(s, 1H, H-2)	6.78	(br, 1H, H-2 Dhba)
6.88	(t, 1H, H-3 Dhba)	6.61	(s, 1H, H-3)	6.69–6.59	(m, 1H, H-3 Dhba)
		3.69	(q, 2H, CH$_2$)	4.53	(q, 1H, CH Nac)
4.66	(q, 1H, CH Nac)	1.22	(t, 3H, CH$_3$)	3.69	(q, 2H, CH$_2$ ethanol)
3.02	(sep, 2H, CH$_2$ Nac)			3.02–2.99	(dd, 2H, CH$_2$ Nac)
2.11	(s, 3H, CH$_3$ Nac)			1.60	(s, 3H, CH$_3$ Nac)
				1.22	(t, 3H, CH$_3$ ethanol)

[a] Proton chemical shift (δ) in ppm unit.
[b] Signal assignment in parenthesis represents the splitting pattern, number of proton, proton location in the compound geometry and splitting distance. Splitting pattern abbreviations: s = singlet, d = doublet, t = triplet, q = quartet, sep = septet, dd = doublet of doublets, br = broad, m = multiplet (complex pattern).

Table 4
Equilibrium constants at various temperatures and I of 0.15 mol/l NaCl[a].

Parameters	Equilibrium constants at different temperature							
	25 °C		37 °C[b]		45 °C		55 °C	
	Dhba	Nac	Dhba	Nac	Dhba	Nac	Dhba	Nac
Dissociation constant								
pK_{a1}	2.68 (2)	3.17 (3)	2.63 (4)	3.18 (2)	2.60 (3)	3.12 (2)	2.54 (1)	3.12 (1)
pK_{a2}	10.11 (2)	9.60 (2)	9.98 (2)	9.48 (5)	9.84 (4)	9.42 (2)	9.81 (4)	9.33 (2)
pK_{a3}	nd[c]	–	13.00 (2)	–	12.72 (1)	–	12.60 (2)	–
σ [d]	1.13	1.06	1.02	1.02	1.05	1.26	1.23	1.09
Binary–stability constant								
$\log_{10} \beta_1$	10.55 (3)	6.53 (7)	10.48 (4)	6.23 (8)	10.25 (2)	6.19 (2)	10.02 (5)	6.05 (5)
$\log_{10} \beta_2$	16.53 (4)	12.11 (2)	16.52 (9)	11.97 (8)	16.51 (7)	11.98 (4)	16.11 (3)	11.91 (4)
σ [d]	1.08	1.34	1.48	1.41	1.40	1.21	1.11	1.19
Ternary–stability constant								
$\log_{10} \beta_T$	16.59 (8)		16.38 (7)		16.02 (5)		15.51 (6)	
σ [d]	1.56		1.55		1.61		1.69	
$\Delta\log_{10} K$	−0.49		−0.33		−0.42		−0.56	
$\log_{10} X$	4.54		4.27		3.55		3.00	

[a] Standard deviations in parentheses at last decimal place represent the standard uncertainties of temperature $u(T) = 0.1$ °C.
[b] Values cited from Refs. [11] and [15], potentiometry method at $I = 0.15$ mol/l NaCl.
[c] Not defined.
[d] Sigma (σ), the goodness of fitting in a system with expectation value of 1.00.
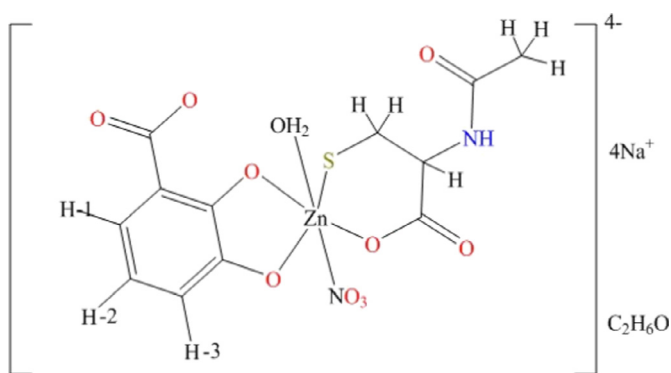
Fig. 5. Proposed structure of zinc ternary complex.

3.4.4. Effect of temperature on thermodynamic parameters

The dissociation constant (pK_a) of Dhba and Nac as well as the stability constant ($\log_{10} \beta$) of their binary and ternary complexes with Zn^{2+} in aqueous solution with $I = 0.15$ mol/l NaCl were determined at different temperatures (25 °C, 37 °C, 45 °C and 55 °C) and the results are presented in Table 4. Particularly for pK_{a3} of Dhba at 25 °C, a big error occurred during refinement thus resulting in undefined value. The error may be caused by the decrease

of the acidity of the ligand Dhba at low temperature resulting in delay in dissociation. The change of acidity is well demonstrated in Table 4 since pK_a value decreased as the temperature was increased. In order to observe the capability of the ligand in preventing the formation of metal hydrolytic species, the hydrolysis constants were included in the determination of $\log_{10} \beta$. No metal hydrolytic species were observed in the systems, indicating that the ligands were capable in preventing their formation (Fig. S1). The $\log_{10} \beta$ of binary and ternary complexes also decrease with increasing temperature indicating that complex is more likely to disassociate at higher temperature.

Additional parameters $\Delta\log_{10} K$ and $\log_{10} X$ were determined with respect to the ternary species, where their values are calculated as:

$$\Delta\log_{10} K = \log_{10} \beta_{Zn(Dhba)(Nac)} - [\log_{10} \beta_{Zn(Dhba)} + \log_{10} \beta_{Zn(Nac)}] \tag{3}$$

$$\log_{10} X = 2\log_{10} \beta_{Zn(Dhba)(Nac)} - [\log_{10} \beta_{Zn(Dhba)2} + \log_{10} \beta_{Zn(Nac)2}] \tag{4}$$

Less negative $\Delta\log_{10} K$ indicates the formation of ternary species is more favorable than that of binary species [6,21]. At all temperatures, the complexes exhibit negative $\Delta\log_{10} K$ value

Table 5
Thermodynamics properties of Dhba, Nac, binary and ternary complexes of Zn.

Species	$-\Delta G$ (kJ/mol)				$-\Delta H$ (kJ/mol)	ΔS (J/K·mol)			
	25 °C	37 °C	45 °C	55 °C		25 °C	37 °C	45 °C	55 °C
H_3Dhba	15.30	15.68	15.84	15.96	8.49	22.85	23.19	23.11	22.78
H_2Dhba	57.72	59.27	59.95	61.64	19.45	128.35	128.39	127.29	128.57
HDhba	–	77.20	77.49	79.17	41.80	–	114.14	112.17	113.88
H_2Nac	18.10	18.89	19.01	19.60	11.24	22.99	24.64	22.68	23.38
HNac	54.81	56.30	57.39	58.62	16.33	129.07	128.89	129.06	128.90
Zn(Dhba)	60.23	62.24	62.44	62.96	33.04	91.19	94.14	92.41	91.18
Zn(Dhba)$_2$	94.37	98.11	100.58	101.23	22.77	240.15	242.91	244.57	239.09
Zn(Nac)	37.28	37.00	37.71	38.02	28.36	29.93	27.86	29.40	29.43
Zn(Nac)$_2$	69.14	71.09	72.98	74.84	11.43	193.56	192.37	193.48	193.24
Zn(Dhba)(Nac)	94.71	97.28	97.59	97.46	65.78	97.04	101.56	100.00	97.64

indicating that the formation of ternary complex is less preferred than binary complex. Such phenomenon probably occurred because of electrostatic effect between the ligands thus lowering the stability of the complex. Meanwhile, for $\log_{10} X$ parameter, the value higher than statistical value ($+0.6$ for all geometries) indicates remarkable stability of ternary complex. All of the ternary complexes exhibit positive $\log_{10} X$ greater than the statistical value. This point out that the secondary ligand (Dhba) prefers to attach at the binary complex Zn(Nac) rather than attach to metal ion. Nac is designated as the primary ligand and Dhba as the secondary ligand since the formation of Nac binary complexes took place at lower pH than that of Dhba binary complexes. The $\log_{10} X$ decreases with increasing temperature, indicating that ternary complex is less stable at higher temperature. This trend is supported by the $\log_{10} \beta$ values which also decreased with increasing temperature.

Thermodynamic properties such as ΔG (Gibbs free energy), ΔH (enthalpy) and ΔS (entropy) provides significant information related to the complex. ΔG can be calculated as:

$$\Delta G = -2.303\, RT \log_{10} \beta \tag{5}$$

ΔH can be determined as the slope of the Van't Hoff plot which is defined as:

$$\log_{10} \beta = \left(\frac{-\Delta H}{2.303R}\right) 1/T + \left(\frac{-\Delta S}{2.303R}\right) \tag{6}$$

Thermodynamic properties of Dhba, Nac as well as the Zn binary and ternary complexes are given in Table 5.

Negative values of ΔG and ΔH in the dissociation of the ligands and chelation of binary and ternary Zn complexes indicate that the reactions are spontaneous and exothermic, so that lower temperature is more favorable for complex synthesis. All ΔS values are positive indicating that complex formation is favorable.

4. Conclusion

Binary and ternary complexes of M/Dhba/Nac were synthesized. FTIR spectra and UV–vis spectra indicate that all complexes have similar structure. The complexes did not increase the scavenging activity of Dhba against DPPH. However in the antimicrobial evaluations against *S. aureus* and *E. coli*, the complexes were found to be more effective than that of Dhba which is caused by the enhancement of hydrophobicity of the complexes. The binary and ternary complexes of Zn gave the best enhancement in antimicrobial activity of Dhba and were characterized further. The binary complex was found to bind metal ion through *ortho* and *meta* $-$O group, which has the molecular structure $C_9H_{11}NNa_2O_9Zn$. The ternary complex was found to bind metal ion through *ortho* and *meta* $-$O group of Dhba, and $-$COO and $-$S of Nac, which has the molecular structure $C_{14}H_{18}N_2Na_4O_{12}SZn$. The formation of binary and ternary complex was found to be spontaneous and exothermic.

Supplementary materials

Supplementary material associated with this article can be found, in the online version, at doi:10.1016/j.jtice.2016.08.003.

References

[1] Penesyan A, Gillings M, Paulsen IT. Antibiotic discovery: combatting bacterial resistance in cells and in biofilm communities. Molecules 2015;20:5286–98.
[2] Williams LB, Haydel SE. Evaluation of the medicinal use of clay minerals as antibacterial agents. Int Geol Rev 2010;52:745–70.
[3] Abbehausen C, Heinrich TA, Abrao EP, Costa-Neto CP, Lustri WR, Formiga ALB, et al. Chemical, spectroscopic characterization, DFT studies and initial pharmacological assays of a silver(I) complex with N-acetyl-ʟ-cysteine. Polyhedron 2011;30:579–83.
[4] Bruckner C, Caulder DL, Raymond KN. Preparation and structural characterization of nickel(II) catecholates. Inorg Chem 1998;37:6759–64.
[5] Bukhari SB, Memon S, Tahir MM, Bhanger MI. Synthesis, characterization and antioxidant activity copper-quercetin complex. Spectrochim Acta Mol Biomol Spectros 2009;71:1901–6.
[6] Dharmaraja J, Esakkidurai T, Subbaraj P, Shobana S. Mixed ligand complex formation of 2-aminobenzamide with Cu(II) in the presence of some amino acids: synthesis, structural, biological, pH-metric, spectrophotometric and thermodynamic studies. Spectrochim Acta Mol Biomol Spectros 2013;114:607–21.
[7] George S, Benny PJ, Kuriakose S, George C, Gopalakrishnan S. Antiprotozoal activity of 2, 3-dihydroxybenzoic acid isolated from the fruit extracts of *Flacourtia inermis Robx*. Asian J Pharm Clin Res 2011;3:237–41.
[8] Juurlink BHJ, Azouz HJ, Aldalati AMZ, Al Tinawi BMH, Ganguly P. Hydroxybenzoic acid isomers and the cardiovascular system. Nutr J 2014;13:63.
[9] Harada H. An investigation of the stability constant of the 2, 3-dihydroxybenzoic acid complex with copper(II). Bull Chem Soc Jpn 1971;44:3459–60.
[10] Kiss T, Kozlowski H, Micera G, Erre LS. Copper(II) complexes of 2, 3-dihydroxybenzoic acid. J Coord Chem 1989;20:49–56.
[11] Santoso SP, Angkawijaya AE, Ismadji S, Ayucitra A, Soetaredjo FE, Lan TNP, et al. Complex formation study of binary and ternary complexes including 2, 3-dihydroxybenzoic acid, N-acetylcysteine and divalent metal ions. J Sol Chem 2016:1–16.
[12] Dean O, Giorlando F, Berk M. N-acetylcysteine in psychiatry: current therapeutic evidence and potential mechanisms of action. J Phsychiatry Neurosci 2011;36:78–86.
[13] Samuni Y, Goldstein S, Dean OM, Berk M. The chemistry and biological activities of N-acetylcysteine. Biochim Biophys Acta 2013;1830:4117–29.
[14] Guzeloglu S, Yalcin G, Pekin M. The determination of stability constant of N-acetyl-L-cysteine chrome, nickel, cobalt and iron complexes by potentiometric method. J Organomet Chem 1998;568:143–7.
[15] Santoso SP, Chandra IK, Soetaredjo FE, Angkawijaya AE, Ju YH. Equilibrium studies of complexes between N-acetylcysteine and divalent metal ions in aqueous solutions. J Chem Eng Data 2014;59:1661–6.
[16] Alam MN, Bristi NJ, Rafiquzzaman M. Review on in vivo and in vitro methods evaluation of antioxidant activity. Saudi Pharm J 2013;21:143–52.
[17] Wiegand I, Hilpert K, Hancock REW. Agar and broth dilution methods to determine the minimal inhibitory concentration (MIC) of antimicrobial substances. Nature Protocols 2008;3:163–75.

[18] Gans P, Sabatini A, Vacca A. Determination of equilibrium constants from spectrophometric data obtained from solutions of known pH: the program pHab. Talanta 1996;43:1739–53.

[19] Nakamoto K. Infrared and Raman spectra of inorganic and coordination compounds. New York: Wiley; 1986.

[20] Shebl M, Ibrahim MA, Khalil SME, Stefan SL, Habib H. Binary and ternary copper(II) complexes of a tridentate ONS ligand derived from 2-aminochromone-3 carboxaldehyde and thiosemicarbazide: synthesis, spectral studies and antimicrobial activity. Spectrochim Acta Mol Biomol Spectros 2013;115:399–408.

[21] Chandra IK, Angkawijaya AE, Santoso SP, Ismadji S, Soetaredjo FE, Ju YH. Solution equilibria studies of complexes of divalent metal ions with 2-aminophenol and 3,4-dihydroxybenzoic acid. Polyhedron 2015;88:29–39.

[22] Abdallah SM, Zayed MA, Mohamed GG. Synthesis and spectroscopic characterization of new tetradentate Schiff base and its coordination compounds of NOON donor atoms and their antibacterial and antifungal activity. Arab J Chem 2010;3:103–13.

[23] Jing P, Zhao SJ, Jian WJ, Qian BJ, Dong Y, Pang J. Quantitative studies on structure-DPPH* scavenging activity relationship of food phenolic acids. Molecules 2012;17:12910–24.

[24] Kitaoka N, Liu G, Masuoka N, Yamashita K, Manabe M, Kodama H. Effect of sulfur amino acids on stimulus-induced superoxide generation and translocation of p47phox and p67phox to cell membrane in human neutrophils and the scavenging of free radical. Clin Chim Acta 2005;353:109–16.

[25] Ozcelik D, Uzun H, Naziroglu M. N-Acetylcysteine attenuates copper overload-induced oxidative injury in brain of rat. Biol Trace Elem Res 2012;147:292–8.

[26] Atmaca S, Gul K, Cicek P. The effect of zinc on microbial growth. Tr J Med Sci 1998;28:595–7.

[27] Popova TP, Alexandrova RI, Tudose R, Mosoarca EM, Costisor O. Antimicrobial activity in vitro of four nickel complexes. Bulg J Agric Sci 2012;18:446–50.

[28] Silhavy TJ, Kahne D, Walker S. The bacterial cell envelope. Cold Spring Harb Perspect Biol 2010;2:1–16.